EASR

Engineering and Applied Science Research

https://www.tci-thaijo.org/index.php/easr/index

Published by the Faculty of Engineering, Khon Kaen University, Thailand

Characterization of Prussian blue-immobilized chitin-coated nylon fibers as adsorbent for cesium ions

Duangkamol Dechojarassri, Sahori Omote, Takanori Minamino, Kensuke Nishida, Tetsuya Furuike and Hiroshi Tamura*

Faculty of Chemistry, Materials and Bioengineering, Kansai University, Osaka, 564-8680, Japan

Received 12 Feb 2018
Accepted 27 April 2018

Abstract

A Prussian blue (PB; KFe)-immobilized chitin-coated nylon (KFe/CT/nylon) fiber was successfully synthesized for the first time. The characteristics of this fiber were compared to that of a KFe-immobilized chitosan-coated rayon (KFe/CTS/rayon) fiber, which shows excellent cesium ion (Cs^+) adsorption and has a high potential for practical use. The aim of producing the KFe/CT/nylon fiber is to study the feasibility of using it instead of a KFe/CTS/rayon fiber to adsorb Cs^+ from contaminated water. CT can not only react with KFe but is also cheaper than CTS; therefore, it is interesting to consider KFe/CT/nylon fiber as an alternative material for Cs^+ adsorption. The interactions between KFe and CT in the nylon fiber or KFe and CTS in the rayon fiber were confirmed via X-ray photoelectron spectroscopy (XPS), X-ray diffraction (XRD), and Fourier transform infrared (FTIR) spectroscopy. The Cs^+ concentration was determined using inductively coupled plasma mass spectrometry (ICP-MS). The Cs^+ adsorption capacity of the KFe/CTS/rayon and KFe/CT/nylon fibers were compared. The Cs^+ adsorption capacity of the KFe/CTS/rayon fiber (90.5%) was found to be significantly higher than that of the KFe/CT/nylon fiber (16.9%) at an initial Cs^+ concentration of 0.67 mg/L.

Keywords: Cesium, Chitin-coated nylon fiber, Chitosan-coated rayon fiber, Prussian blue, Adsorption

1. Introduction

The contamination of water with radioactive cesium (Cs) is a serious problem because Cs can be accumulated in the soft tissue of humans. One of the major accidents that raised the urgency of treating such contaminated water was the damage of the Fukushima Daiichi Nuclear Power Plant after the earthquake in East Japan. Radioactive Cs can be removed via adsorption or absorption using various materials, including zeolite or zeolite complexes [1-5], clinoptilolite-rich tuffs [6], and hybridized microporous silica-based functional materials [7]. In addition, iron composites or the functionalization of iron complexes has been proposed for Cs^+ removal from contaminated water. Such materials include metal ferrocyanide-anion exchange resins [8], cobalt ferrocyanide-impregnated organic anion exchangers [9], cobalt ferrocyanide-impregnated polymer-chain-grafted fibers [10], potassium iron(III) hexacyanoferrate(II) support on activated carbon [11], potassium zinc hexacyanoferrate [12], Prussian blue (PB) composite material, and materials functionalized with PB [13-17].

PB [$(Fe_7(CN)_{18}$; iron(III) hexacyanoferrate(II)], also called iron blue, Berlin blue, Paris blue or KFe is a dark blue pigment used in paints and it could be synthesized by the oxidation of iron. The KFe ions can be exchanged with soft metal cations, including Cs^+. The hydration radius of Cs^+ is close to the cage size of KFe crystals, making KFe a good candidate for the removal of Cs^+-contaminated water via adsorption. However, the recovery of adsorbents after Cs^+ adsorption must be considered. Therefore, KFe has been applied in various forms, such as granules [18], sponges [13, 16], fibers [17], and magnetic materials [14-15]. Batch adsorption was been performed, and Cs^+ removal through the continuous flow of contaminated water in a fixed-bed system was also investigated [6].

The recent trend of using biomaterials as adsorbents has been extensively acknowledged in the literature. Among the large number of biomaterials that are studied, chitin (CT) is an important resource because it is the second most abundant polysaccharide in nature [19]. It can be derived from crabs, shrimp shells, insect cuticles, and fungal cell walls by decalcification and alkali treatment. The deacetylation of CT results in chitosan (CTS), another well-known biopolymer. Both CT and CTS are biocompatible, biodegradable, and nontoxic materials and can thus be applied in many fields, e.g., as adsorbent in the treatment of contaminated water. CT and its composite can be used to remove arsenic [As(III)], copper, and hazardous dyes from aqueous solutions [20-22]. Moreover, CT and CTS perform even better when coupled with KFe [16-17]. It was reported that Cs^+ can be removed by using KFe/CT sponges. However, these sponges were obtained by synthesizing a KFe/CTS composite, which was re-acetylated to yield KFe/CT sponges [16].

*Corresponding author. Tel.: +81 6 6368 0871
Email address: tamura@kansai-u.ac.jp
doi: 10.14456/easr.2018.23

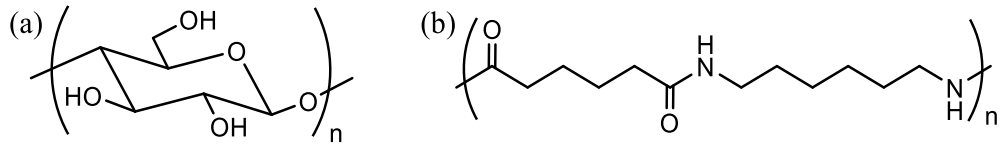

Figure 1 Chemical structures of (a) rayon and (b) nylon 6,6

In our previous research, rayon fibers coated with CTS and immobilized with KFe were successfully produced and the adsorption and desorption behaviors of Cs^+ were investigated using these fibers [17]. Fibers were chosen because of their high surface area-to-volume ratio. To date, there has been no research on KFe/CT fibers for Cs^+ removal. Therefore, this study aimed to prepare KFe/CT composite fibers for removing Cs^+ from water. According to our previous work, CTS can react with modified rayon fiber through KIO_4 [17]. On the other hand, CT cannot react with rayon fiber because its chemical structure differs from that of CTS; therefore, another support material had to be chosen, which is nylon 6,6.

Rayon is made from purified cellulose, which can be obtained from natural fibers such as silk, wool, cotton, or linen. As, in the production of rayon fiber, chemicals are used to convert the cellulose into a soluble compound and the dissolved cellulose is forced through a spinneret to produce filaments, it is considered a semi-synthetic fiber [23]. In this work, viscose rayon ($(C_6H_{10}O_5)_n$) was used as the supporter fiber for CTS. Viscose rayon is conventionally made from cellulose obtained from cotton linters or softwoods. The cellulose is separated, purified, soaked in sodium hydroxide, and then dried. The obtained fiber is mixed with carbon disulfide, and finally it is extruded through a spinneret to produce viscose rayon [24]. Unlike rayon, nylon 6,6 ($(C_{12}H_{22}N_2O_2)_n$) is a synthetic fiber, which is commercially available. In addition, it has many advantages such as high strength because of hydrogen bonding, a high melting point, and high crystallinity. Compared to other grades of nylon, this higher crystallinity of nylon 6,6 results in higher stiffness, higher density, higher tensile and yield stress, as well as higher chemical and abrasion resistance [25]. The chemical structures of rayon and nylon 6,6 are shown in Figures 1(a) and 1(b), respectively. In terms of the chemical structure of rayon and nylon, rayon consists of a ring-based structure while nylon contains a linear chain structure. Considering these factors, the synthesis and characterization of CT-coated nylon fibers immobilized with KFe (KFe/CT/nylon fiber), which has not been previously reported, is of considerable interest and is worth investigating. Therefore, in this work, the production of KFe/CT/nylon fibers was investigated for use as an adsorbent for Cs^+ removal. In addition, its characteristics were compared with those of CTS-coated rayon fibers immobilized with KFe (KFe/CTS/rayon fiber).

2. Materials and methods

2.1 Materials

Nylon 6,6 (EXTRA V-500 No. 1) was purchased from Sanyo Nylon Co., Ltd. (Japan). α-CT (DAC: 1.2), CTS FH-80 (DAC: 85.7; 280 mPa·s), and CTS FL-80 (DAC: 84.7; 5 mPa·s) were obtained from Koyo Chemical Co., Ltd. (Japan). Spun yarn 30^S rayon (3212 30NJHB12/5 CO grade) was obtained from Omikenshi Co., Ltd. (Japan). PB ($KFe[Fe(CN)_6]$), used as a source of KFe, was obtained from Hitachi Zosen Corporation (Japan). Potassium periodate (KIO_4) and Cs^+ standard solution were purchased from Wako Pure Chemical Industries, Ltd. (Japan). All chemicals were directly used without any purification.

2.2 Preparation of woven KFe/CT/nylon and KFe/CTS/rayon fibers

To create effective radioactive Cs^+ adsorbents and investigate the ability to scale up the production of these adsorbents in the future, the fibers were interlaced with woven fibers using three lines of 16 bobbins (30^S//3×16) for either KFe/CT/nylon or KFe/CTS/rayon fibers. These fibers were manufactured with an interlaced machine (Kokubun Ltd., Japan). The interlacing conditions were set according to those set in a previous study [17]: an interlacing speed of 30.06–30.99 rpm and a gear ratio of the delivery side to the knit side of 60:50. The fiber preparation scheme and the interlacing machine are shown in Figures 2 and 3, respectively.

To prepare the KFe/CT/nylon fiber, 1% (w/v) CT and 4% (w/v) nylon 66 were prepared by dissolving CT and nylon 66 in saturated $CaCl_2{\cdot}2H_2O$/MeOH. To prepare saturated $CaCl_2{\cdot}2H_2O$/MeOH, 850 ml of MeOH and 1050 g of $CaCl_2{\cdot}2H_2O$ powder were placed in a three-necked flask and stirred while distilling at 110°C for 24 h. Subsequently, the solution was cooled to room temperature to precipitate excess $CaCl_2$. Next, suction filtration was performed. Based on these steps, saturated $CaCl_2{\cdot}2H_2O$/MeOH was obtained. The CT and nylon 66 solutions were then mixed at a ratio of 3:1 to obtain a 0.75% CT–1% nylon 66 solution. The woven nylon fiber (30^S//3×16) was then soaked in the prepared solution and calcium was removed by immersing the fiber in 1% NaOH in MeOH. Then the fiber was immersed in 1% HCl/MeOH for 2 min. The CT-coated nylon fiber was brushed, dried, 0.5 g dried CT-coated nylon fiber was then immersed in a KFe solution (100 mL; 2 mM) and stirred at 100°C for 1 h. The fiber was washed with water and dried to obtain the KFe/CT/nylon fiber.

The KFe/CTS/rayon fiber was prepared according to the previous report [17]; the rayon fiber (5 g) was soaked in a KIO_4 solution (1 mg/mL) at 60°C for 1 h. The fiber was washed with water and soaked in a CTS solution [3% (w/v)] at 60°C for 2 h. The rayon fiber was immobilized with KFe by soaking it in a KFe solution (400 mL; 2 mM) at 100°C for 1 h. The KFe/CTS/rayon fiber was then interlaced to obtain 30^S//3×16 KFe/CTS/rayon fibers. An excess KFe concentration was used in this work for both types of fibers. After soaking in KFe solution, the KFe/CT/nylon fiber or KFe/CTS/rayon fiber was then removed, and the amount of KFe immobilized on the fibers was calculated by measuring the remaining KFe concentration in the soaking solution against a calibration curve via UV-vis spectroscopy (Hitachi U-2910, Japan). The absorbance was measured at a wavelength of 207 nm.

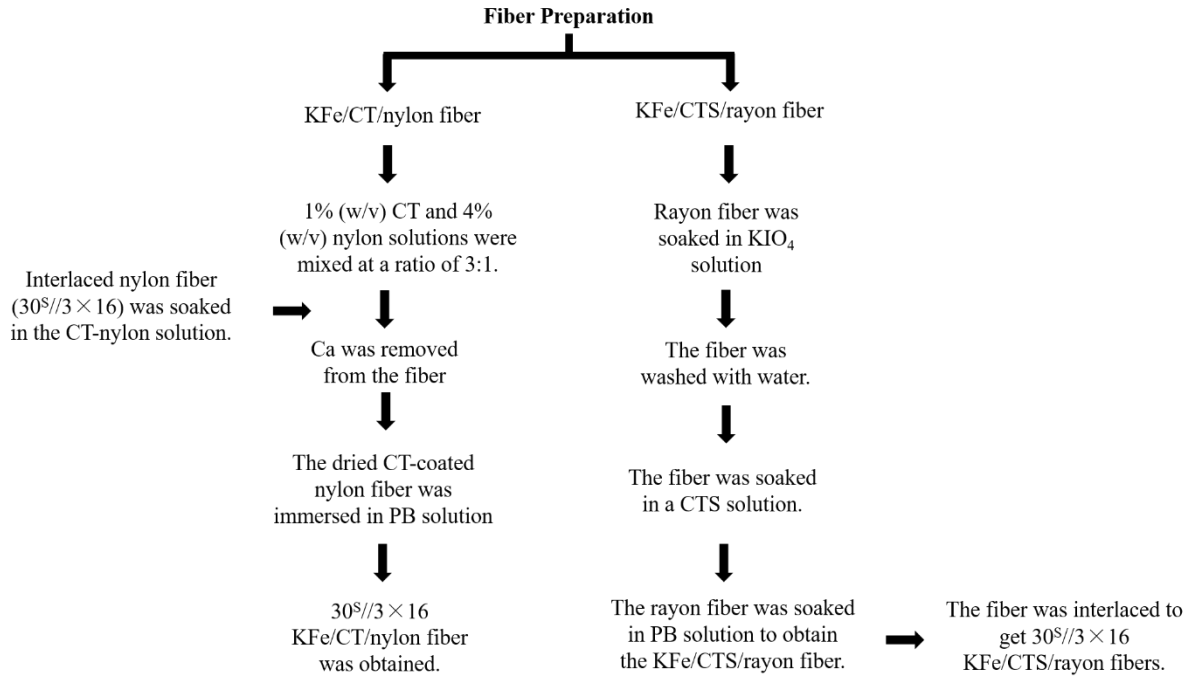

Figure 2 Fiber preparation scheme

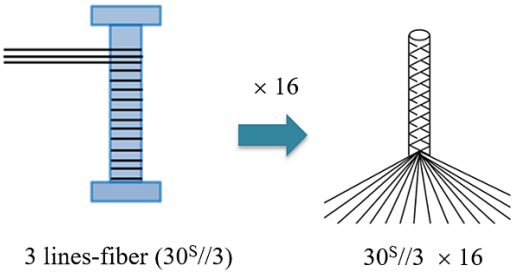

Figure 3 Interlacing machine

2.3 Characterization of the KFe/CT/nylon and KFe/CTS/rayon fibers

The presence of KFe on the surface of both the KFe/CT/nylon and KFe/CTS/rayon fibers was confirmed using X-ray photoelectron spectroscopy (XPS; Shimazu ESCA3400, Japan) with monochromatic Al Kα radiation (1486.7 eV) and a non-monochromated Mg Kα X-ray source (1253.6 eV). X-ray Diffraction (XRD, RAPID II, Rigaku Corporation, Japan) was carried out with a Cu counter cathode (0.15 Å), angle ω = 90°, Φ = x = 0°, measuring time of 300 s, and measurement range 0–45°. Fourier transform infrared (FTIR) spectroscopy (IR-4200, JASCO Corporation, Japan) was carried out with KBr pellets at 60°C and a scanning frequency of 4,000–500 cm^{-1}.

2.4 Cs^+ adsorption capacity of the KFe/CT/nylon and KFe/CTS/rayon fibers

For the Cs^+ adsorption test, 0.25 g of each fiber was immersed in a Cs^+ solution (50 mL; 0.67 mg/L) and shaken at 25°C and 160 rpm for 1 h. The Cs^+ concentration was measured using inductively coupled plasma mass spectrometry (ICP-MS) at a wavelength of 455 nm. The Cs^+ adsorption percentage and capacity were obtained using a calibration curve and calculated using Equations (1) and (2):

$$Cs^+ \text{ adsorption percentage } (\%) = \frac{C_i - C_f}{C_i} \times 100 \quad (1),$$

$$Cs^+ \text{ adsorption capacity } (mg/g) = \frac{(C_i - C_f) \times V}{W} \quad (2),$$

where C_i and C_f are the initial and final Cs^+ concentrations (mg/L), respectively, and V and W are the volume of the Cs^+ solution (L) and the amount of fiber used in the adsorption process (g), respectively.

3. Results and discussion

3.1 Characterization of the KFe/CT/nylon and KFe/CTS/rayon fibers

The presence of KFe on the surfaces of both the KFe/CT/nylon and KFe/CTS/rayon fibers was confirmed via XPS (Figure 4). A significant peak was observed at a binding energy (BE) of ~708.8 eV, which corresponded to the Fe 2p region (700–740 eV) [26-27]. In addition, a specific BE peak observed at 710 eV corresponded to Fe $2p^{3/2}$, which is indicative of the Fe(III) oxidation state [26]. In both the KFe/CT/nylon and KFe/CTS/rayon fibers, BE peaks at ~710 eV were observed. The BE peak of the KFe/CT/nylon fiber shifted from 708.9 to 709.5 eV, while that of the KFe/CTS/rayon fiber shifted from 708.8 to 711.5 eV. Based on the comparison of the BE intensities of the KFe/CT/nylon and KFe/CTS/rayon fibers, the BE intensities of the KFe/CTS/rayon fiber at ~710 eV were found to be higher than those of the KFe/CT/nylon fiber. The larger shift and higher intensity of the BE peak of the KFe/CTS/rayon fiber compared with those of the KFe/CT/nylon fiber indicates a higher KFe immobilization of CTS/rayon fiber compared with CT/nylon fiber.

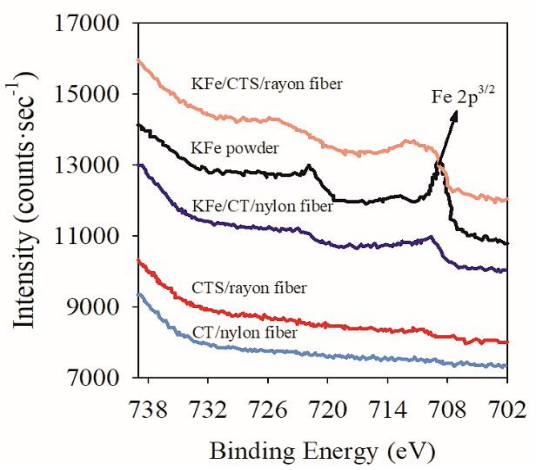

Figure 4 XPS Fe 2p spectra of KFe/CT/nylon fiber and KFe/CTS/rayon fiber

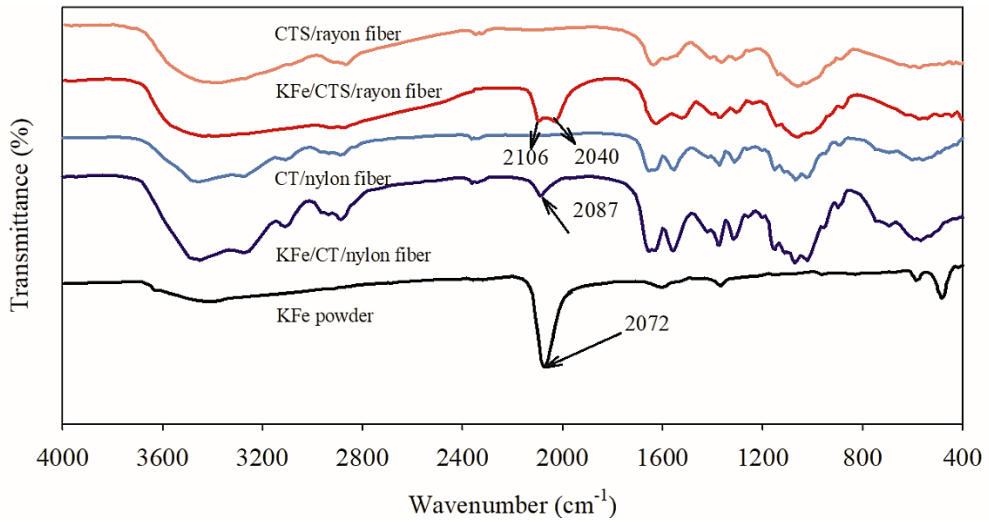

Figure 5 FTIR spectra of KFe/CT/nylon fiber and KFe/CTS/rayon fiber

The FTIR spectra of the KFe/CT/nylon and KFe/CTS/rayon fibers are shown in Figures 5. Based on the absorption band at 2072 cm^{-1}, common KFe characteristics were observed due to the stretching vibration of the C≡N group [28]. In the FTIR spectrum of KFe-immobilized CT/nylon, a peak at 2087 cm^{-1} was observed. In the FTIR spectrum of KFe/CTS/rayon fiber, the peaks at 2106 and 2040 cm^{-1} are attributed to the degenerative deformation and torsional vibration of NH_3^+ [29] and the stretching vibration of the C≡N group [28], respectively. These peaks around 2072 cm^{-1} confirm that there are interactions between KFe and the CT/nylon fiber or CTS/rayon fiber. Based on the transmittance of the KFe peak, the transmittance of the KFe/CTS/rayon fiber was found to be higher than that of the KFe/CT/nylon fiber. These results confirmed that KFe reacts with the CTS/rayon fiber better than with the CT/nylon fiber.

The XRD patterns exhibit sharp KFe/CT/nylon fiber peaks and broad KFe/CTS/rayon fiber peaks (Figure 6). In addition, the XRD pattern of KFe/CT/nylon fiber was rather similar to that of CT/nylon fiber. The peak intensities of all peaks of the KFe/CT/nylon fiber were smaller than those of the CT/nylon fiber, confirming that the degree of crystallinity was lowered. Moreover, a comparison with the KFe powder pattern indicated that the intensities of the KFe/CT/nylon fiber were also smaller than those of KFe powder. These results indicate that the amount of KFe immobilized on the CT/nylon fiber is quite small. Considering the XRD pattern of the KFe/CTS/rayon fiber, the peaks corresponding to 2θ = 17.4°, 24.6°, 35.2°, 39.4°, and 43.4° are similar to peaks found in the KFe powder pattern and the XRD pattern of the ITO electrode modified with CTS nanofiber/KFe nanoparticles [30]. In conclusion, the fact that all peaks are similar for the KFe/CTS/rayon fiber and KFe powder confirms that the crystallinities of the KFe/CTS/rayon fiber and KFe are similar.

The chemical reactions of the KFe/CTS/rayon fiber are shown in our previous work [17]. The rayon fibers were first oxidized using KIO_4 to cleave the C2–C3 bond of the glucose residues, affording aldehydes at the C2 and C3 positions. The resulting aldehydes formed an amido linkage with the amino group of CTS upon treatment with the CTS solution. Finally, the KFe/CTS/rayon fiber was obtained after treatment with the KFe solution, where KFe was immobilized by cation exchange from K^+ to NH^{3+} [17]. In contrast to the KFe/CTS/rayon fiber, the chemical interaction of KFe and CT in the KFe/CT/nylon fiber could not be identified. To the best of our knowledge, to date, there is only one study on KFe/CT sponges for Cs^+ recovery [16]. As already mentioned in the Introduction section, the KFe/CTS composite was synthesized first and then re-acetylated to

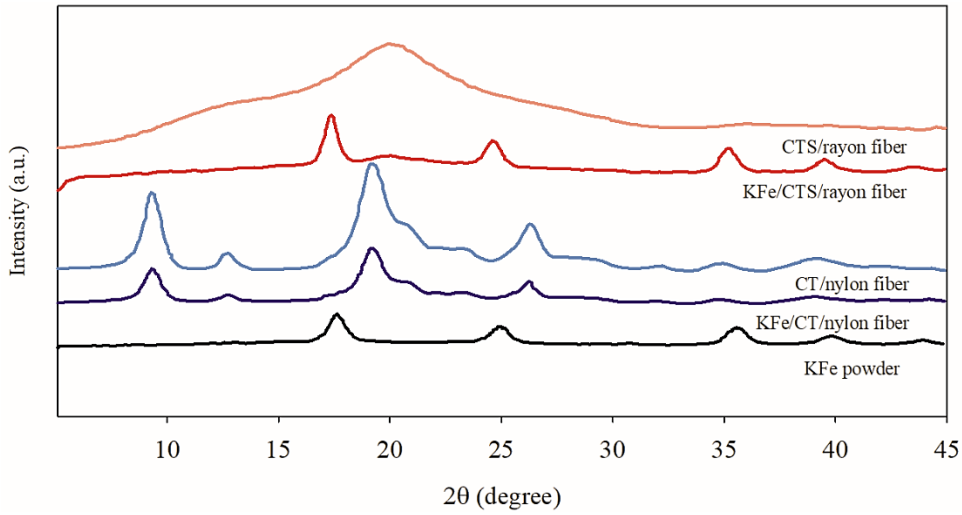

Figure 6 XRD patterns of KFe/CT/nylon fiber and KFe/CTS/rayon fiber

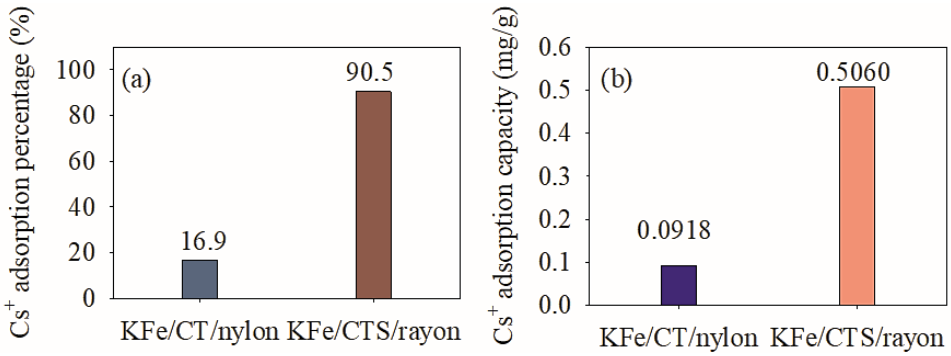

Figure 7 Cs^+ adsorption of fibers: (a) percentage and (b) capacity (mg/g)

obtain KFe/CT sponges. Therefore, the reaction between CT and KFe was not studied in a previous study [16].

3.2 Cs^+ adsorption results obtained using the KFe/CT/nylon and KFe/CTS/rayon fibers

As previously mentioned, after synthesis, the amount of excess KFe was measured using UV-Vis spectrophotometry; thus the amount of the KFe on CT/nylon fiber and CTS/rayon fiber can be calculated. It was found that the amounts of KFe on the CT/nylon fiber and CTS/rayon fibers were 0.55 and 16.6 μmol/g, respectively. The Cs^+ adsorption percentage and capacity when 0.25 g of each fiber was used in a Cs^+ solution (50 mL) with an initial Cs^+ concentration of 0.67 mg/L at 160 rpm for 1 h, are shown in Figures 7. The Cs^+ adsorption percentage, capacity (mg/g) and capacity (μmol/g) of the KFe/CTS/rayon fiber (30S//3×16) were 90.5%, 0.5060 mg/g and 3.81 μmol/g, respectively, approximately five times higher than the Cs^+ adsorption capacity of the KFe/CT/nylon fiber which was 0.0918 mg/g (0.69 μmol/g). This was because the KFe amount of the CTS/rayon fiber was higher than that of the CT/nylon fiber. Considering the results from the XPS spectra (Figure 4) and FTIR spectra (Figure 5), a small change in the binding energy/environment/complexation/chemical bonding of KFe is observed when immobilized on the CT/nylon fiber, whereas significant changes are found when immobilized on the CTS/rayon fiber. These results imply that there are either differing chemical interactions, differing complexations, or modifications of the KFe structure/composition, which may be related to the different structures of either CT/CTS or nylon/rayon. The observations herein partly explain the difference in adsorption capacity between the CTS/rayon fiber and KFe/CTS/rayon fiber (30S//3×16) (Figure 7).

In this work, the preparation method for KFe/CTS/rayon fiber was the same as previously reported [17], but the interlacing of the fiber was different. Here, the KFe/CTS/rayon fiber (30S//3×16) was obtained by using three lines of fiber, while in our previous work, either two or four lines were used to obtain the woven fibers, which were KFe/CTS/rayon fibers (30S//2×16) and KFe/CTS/rayon fibers (30S//4×16), respectively. In addition, those woven fibers were used to adsorb radioactive Cs (Bq/g) whereas here, the KFe/CTS/rayon fiber (30S//3×16) was used as an adsorbent for Cs^+ from a CsCl solution. Therefore, the adsorption capacity of the KFe/CTS/rayon fiber (30S//3×16) cannot be compared to that of woven (30S//2×16) and (30S//4×16) fibers [17]. However, when comparing the adsorption capacity of the KFe/CTS/rayon fiber (30S//3×16) to that obtained in other studies, it was found that when using an 81.8-mg sponge to adsorb Cs^+ (1 mL) with an initial Cs^+ concentration about 93.6 mg/L, the concentration remaining after 1 h was 0.1 mg/L. Based on Eq. (2), the adsorption capacity was calculated to be 1.1430 mg/g (8.60 μmol/g) dry sponge, which was higher than those of KFe/CT/nylon fiber and KFe/CTS/rayon fiber (30S//3×16). In their study, 1 mL of Cs^+ solution was directly dropped onto a 81.8-mg sponge, which enabled Cs^+ to come in contact with KFe, resulting in a higher adsorption capacity compared to our fiber [16]. However, when 2 g of the KFe/CTS/rayon fiber was used

without interlacing in Cs^+ removal process with an initial concentration of 400 ppm (100 mL) for 1 h, the adsorption capacity of the KFe/CTS/rayon fiber was increased to be 2.206 mg/g (16.6 μmol/g) which was significantly higher than those of interlaced fibers. This was because the interlaced fiber had a relatively high density, which allowed Cs^+ to penetrate into the fiber structure.

4. Conclusions

In this work, woven KFe/CT/nylon fibers were successfully prepared and its Cs^+ adsorption capacity was tested to study the feasibility of using them instead of KFe/CTS/rayon fibers. Herein, their characteristics were compared to those of KFe/CTS/rayon fibers (30S//3×16). The Cs^+ adsorption percentage of the interlaced KFe/CTS/rayon fiber (90.5%) was significantly higher than that of the interlaced KFe/CT/nylon fiber (16.9%) at an initial Cs^+ concentration of 0.67 mg/L, and this is owing to a higher amount of KFe on the CTS/rayon fiber. The interactions between KFe and CT in the nylon fiber or KFe and CTS in the rayon fiber were confirmed via XPS, XRD, and FTIR spectroscopy. Differing chemical interactions or complexations or a modification of the KFe structure/composition involving the different structures of either CT/CTS or nylon/rayon may be the main reason why different KFe amounts are immobilized on the different supports. These results reveal that the KFe/CTS/rayon fiber is more suitable than the KFe/CT/nylon fiber as an absorbent for Cs^+ removal from contaminated water. However, this does not consider any economic or environmental factors.

5. Acknowledgements

This work was financially supported by Private University Research Branding Project, MEXT, 2016–2020. and in part by the Kansai University Outlay Support for Establishing Research Centers, 2016−2017. ‘Development and application of biocompatible polymer materials having sol-gel transition’.

6. References

[1] Kawamura F, Motojima K. Using copper hexacyanoferrate (II) impregnated zeolite for cesium removal from radioactive liquid waste. J Nucl Tech. 1982;58:242-6.

[2] Jarai M, Deng Y, Markus F, Harsh JB. Cesium incorporation and diffusion in cancrinite, sodalite, zeolite, and allophane. Micropor Mesopor Mat. 2005;86:277-86.

[3] El-Naggar MR, El-Kamash AM, El-Dessouky MI, Ghonaim AK. Two-step method for preparation of NaA-X zeolite blend from fly ash for removal of cesium ions. J Hazard Mater. 2008;154:963-72.

[4] Munthali MW, Johan E, Aono H, Matsue N. Cs^+ and Sr^{2+} adsorption selectivity of zeolites in relation to radioactive decontamination. J Asian Ceram Soc. 2015;3:245-50.

[5] Mimura H, Yokota K, Akiba K, Onodera Y. Alkali hydrothermal synthesis of zeolites from coal fly ash and their uptake properties of cesium ion. J Nucl Sci Technol. 2001;38:766-72.

[6] Cortés-Martínez R, Olguín MT, Solache-Ríos M. Cesium sorption by clinoptilolite-rich tuffs in batch and fixed-bed systems. Desalination. 2010;258:164-70.

[7] Zhang A, Li Y, Dai Y, Xu L. Development of a new simultaneous separation of cesium and strontium by extraction chromatograph utilization of a hybridized macroporous silica-based functional material. Sep Purif Technol. 2014;127:39-45.

[8] Watari K, Imai K, Ohmomo Y, Muramatsu Y, Nishimura Y, Izawa M, Baciles LR. Simultaneous. Adsorption of Cs-137 and I-131 from water and milk on “metal ferrocyanide-anion exchange resin". J Nucl Sci Technol. 1988;25:495-9.

[9] Valsala TP, Roy SC, Shah JG, Gabriel J, Raj K, Venugopal V. Removal of radioactive caesium from low level radioactive waste (LLW) streams using cobalt ferrocyanide impregnated organic anion exchanger. J Hazard Mater. 2009;166:1148-53.

[10] Ishihara R, Fujiwara K, Harayama T, Okamura Y, Uchiyama S, Sugiyama M, Someya T, Amakai W, Umino S, Ono T, Nide A, Hirayama Y, Baba T, Kojima T, Umeno D, Saito K, Asai K and Sugo T. Removal of cesium using cobalt-ferrocyanide-impregnated polymer-chain-grafted fibers. J Nucl Sci Technol. 2011;48:1281-4.

[11] Kawatake K, Shigemoto N. Preparation of potassium iron(III) hexacyanoferrate(II) supported on activated carbon and Cs uptake performance of the adsorbent. J Nucl Sci Technol. 2012;49:1048-56.

[12] Takahashi A, Kitajima A, Parajuli D, Hakuta Y, Tanaka H, Ohkoshi S, Kawamoto T. radioactive cesium removal from ash-washing solution with high pH and high K^+-concentration using potassium zinc hexacyanoferrate. Chem Eng Res Des. 2016;109:513-8.

[13] Hu B, Fugetsu B, Yu H, Abe Y. Prussian blue caged in spongiform adsorbents using diatomite and carbon nanotubes for elimination of cesium. J Hazard Mater. 2012;217-218:85-91.

[14] Yang H, Li H, Zhai J, Sun L, Zhao Y, Yu H. Magnetic Prussian blue/graphene oxide nanocomposites caged in calcium alginate microbeads for elimination of cesium ions from water and soil. Chem Eng J. 2014;246:10-9.

[15] Yang H, Jang S, Hong SB, Lee K, Roh C, Huh YS, Seo B, Prussian blue-functionalized magnetic nanoclusters for the removal of radioactive cesium from water. J Alloy Compd. 2016;657:387-93.

[16] Vincent C, Barré Y, Vincent T, Taulemesse J, Robitzer M, Guibal E. Chitin-Prussian blue sponges for Cs (I) recovery: from synthesis to application in the treatment of accidental dumping of metal-bearing solutions, J. Hazard. Mater. 2015;287:171-9.

[17] Dechojarassri D, Asaina S, Omote S, Nishida K, Furuike T, Tamura H. Adsorption and desorption behaviors of cesium on rayon fibers coated with chitosan immobilized with Prussian blue. Int J Biol Macromol. 2017;104:1509-16.

[18] Chen G, Chang Y, Liu X, Kawamoto T, Tanaka H, Kitajima A, Parajuli D, Takasaki M, Yoshino K, Chen M, Lo Y, Lei Z, Lee D. Prussian blue (PB) granules for cesium (Cs) removal from drinking water. Sep Purif Technol. 2015;143:146-51.

[19] Knorr D. Use of chitinous polymers in food—A challenge for good research and development. Food Technol-Chicago. 1984;38:85-97.

[20] Yang R, Su Y, Aubrecht KB, Wang X, Ma H, Grubbs RB, Hsiao BS, Chu B. Thiol-functionalized chitin nanofibers for As (III) adsorption. Polymer. 2015;60:9-17.

[21] Labidi A, Salaberria AM, Fernandes SCM, Labidi J, Abderrabbaa M. Adsorption of copper on chitin-based materials: kinetic and thermodynamic studies. J Taiwan Inst Chem E. 2016;65:140-8.
[22] Wawrzkiewicz M, Bartczak P, Jesionowski T. Enhanced removal of hazardous dye form aqueous solutions and real textile wastewater using bifunctional chitin/lignin biosorbent. Int J Biol Macromol. 2017;99:754-64.
[23] Kauffman GB. Rayon: The first semi-synthetic fiber product. J Chem Educ. 1993;70:887-93.
[24] Brinsko KM. Sparenga S, King M. The effects of environmental exposure on the optical, physical, and chemical properties of manufactured fibers of natural origin. J Forest Econ. 2016;61:1215-27.
[25] Vagholkar PK. Nylon (Chemistry, Properties and Uses). Int J Recent Sci Res. 2016;5:349-51.
[26] Guivar JAR, Sanches EA, Bruns F, Sadrollahi E, Morales MA, López EO, Litterst FJ. Vacancy ordered *gamma*-Fe_2O_3 nanoparticles functionalized with nanohydroxyapatite: XRD, FTIR, TEM, XPS and Mössbauer studies. Appl Surf Sci. 2016;389:721-34.
[27] Liu H, Wei G, Xu Z, Liu P, Li Y. Quantitative analysis of Fe and Co in co-substituted magnetite using XPS: The application of non-linear least squares fitting (NLLSF). Appl Surf Sci. 2016;389:438-46.
[28] Arun T, Prakash K, Kuppusamy R, Justin Joseyphus R. Magnetic properties of Prussian blue modified Fe_3O_4 nanocubes. J Phys Chem Solids. 2013;74:1761-8.
[29] Akhtar F, Podder J. A study on growth, structural, optical and electrical characterization of L-alanine single crystal for optoelectronic devices. Res J Phys. 2012;6:31-40.
[30] Shan Y, Yang G, Gong J, Zhang X, Zhu L, Qu L. Prussian blue nanoparticles potentiostatically electrodeposited on indium tin oxide/chitosan nanofibers electrode and their electrocatalysis towards hydrogen peroxide. Electrochim Acta. 2008;53: 7751-5.